A Cleavable Crosslinking Strategy for Commodity Polymer Functionalization and Generation of Reprocessable Thermosets

Liting Bi, Benjamin Godwin, Dr. Miranda J. Baran, Dr. Rashid Nazir, and Prof. Jeremy E. Wulff

2023

Zitierweise: *Angew. Chem. Int. Ed.* **2023**, *62*, e202304708
doi.org/10.1002/anie.202304708

Polymer Functionalization

A Cleavable Crosslinking Strategy for Commodity Polymer Functionalization and Generation of Reprocessable Thermosets

*Liting Bi, Benjamin Godwin, Miranda J. Baran, Rashid Nazir, and Jeremy E. Wulff**

Abstract: Covalently crosslinked polymeric materials, known as thermosets, possess enhanced mechanical strength and thermal stability relative to the corresponding uncrosslinked thermoplastics. However, the presence of covalent inter-chain crosslinks that makes thermosets so attractive is precisely what makes them so difficult to reprocess and recycle. Here, we demonstrate the introduction of chemically cleavable groups into a *bis*-diazirine crosslinker. Application of this cleavable crosslinker reagent to commercial low-functionality polyolefins (or to a small-molecule model) results in the rapid, efficient introduction of molecular crosslinks that can be uncoupled by specific chemical inputs. These proof-of-concept findings provide one potential strategy for circularization of the thermoplastic/thermoset plastics economy, and may allow crosslinked polyolefins to be manufactured, used, reprocessed, and re-used without losing value. As an added benefit, the method allows the ready introduction of functionality into non-functionalized commodity polymers.

Introduction

The annual global production of thermoset polymers is over 65 million tons and comprises about 18% of polymeric materials manufactured today.[1] Addition of covalent crosslinks into polymer networks gives the resulting thermoset enhanced tensile strength, as well as thermal and chemical resistance.[2a] However, this comes at the expense of reprocessability and recyclability. Transforming thermoplastics into thermosets limits the possibility of mechanical reprocessing (melt-and-remould) because the crosslinked structures preclude flow, even at elevated temperatures.[2b] Consequently, most thermosets are incinerated or landfilled after their useful lifetimes.[3,4a] Existing strategies to create reprocessable thermosets have focused on the incorporation of stimuli-triggered degradation or dynamic interactions such as the installation of silyl ether linkages within polydicylopentadiene,[5] carbamate exchange in polyurethane foams,[6] reversible enamine linkages in polydiketoenamines,[7] and boronic ester hydrolysis in vitrimers.[8] None of these methods, however, combine on-demand crosslinking with the ability to uncouple the key inter-chain bond, and most require that bespoke polymer substrates be synthesized, rather than permitting the upgrading of existing, commodity polymer materials.

Traditional crosslinking methods include rubber vulcanization,[9] silicone hydrosilylation[10] and epoxy resin polyamine curing.[11] However, low-functionality polymers such as polyethylene and polypropylene (the most widely produced polymers in the world) lack intrinsically reactive functional groups for crosslinking. As a result, industrial polyethylene crosslinking involves either high-energy radiation (γ rays or electron beams) or peroxide-induced radical reactions. Both methods are poorly controlled, and are generally unsuitable for polypropylene (and even for certain forms of polyethylene) due to competing chain-scission events.[12]

Recently, trifluoromethyl aryl diazirines have shown promising efficacy in polymer crosslinking[13] and photopatterning applications.[14] Upon exposure to heat or light, the strained diazirine heterocycle loses a molecule of nitrogen gas (N_2) to generate a highly reactive carbene, which in turn can insert into neighboring C–H bonds.[15] Thus, the use of *bis*-, *tetrakis*-, or *poly*-diazirines provides a convenient and practical method to rationally install molecular crosslinks into commercial polyolefins without the risk of competing fragmentation reactions, and without any requirement for functional groups to be already present along the polymer chain.[13b,16] Recent structure-function studies revealed that trifluoromethyl aryl diazirines bearing electron-rich aryl groups were much more efficient at undergoing C–H insertion than the corresponding electron-neutral or electron-poor systems.[17a] This in turn led to the design of a prototypical, electronically optimized *bis*-diazirine crosslinker containing aryl ether linkages, which showed improved performance in crosslinking both polymers and small-molecule models.[17b]

In the current work, we describe the design, synthesis, and testing of a series of electronically optimized *bis*-diazirines that incorporate chemically cleavable functional groups (Figure 1). These include a carbonate, an oxalate, and a silyl ether, each of which can undergo bond cleavage/

[*] L. Bi, B. Godwin, Dr. R. Nazir, Prof. J. E. Wulff
Department of Chemistry, University of Victoria
Victoria, British Columbia V8W 2Y2 (Canada)
E-mail: wulff@uvic.ca
Dr. M. J. Baran
XlynX Materials, Inc.
Victoria, British Columbia V8P 5C2 (Canada)

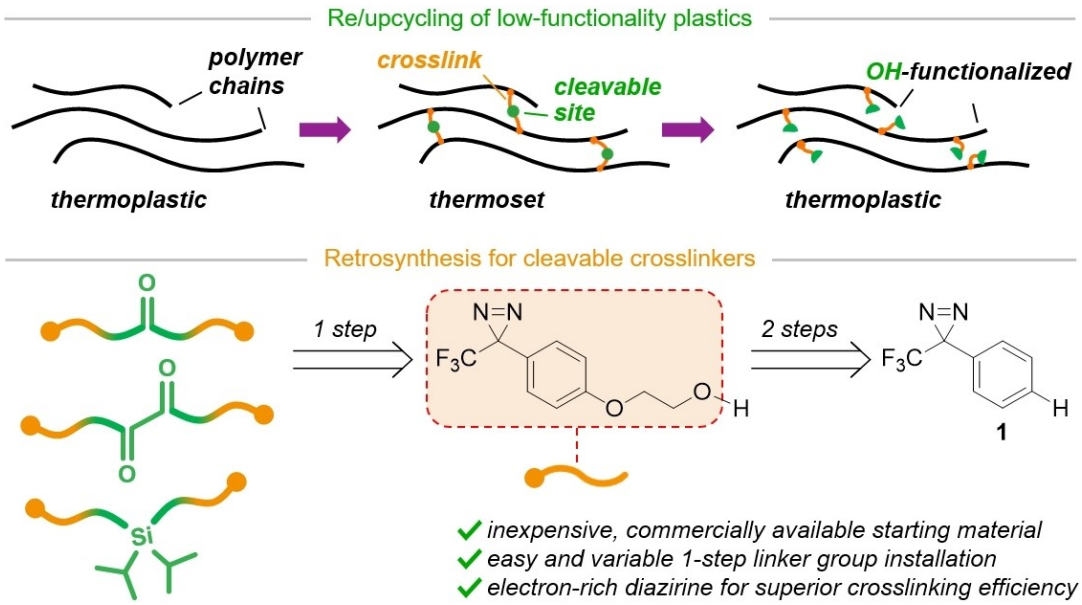

Figure 1. A broadly applicable, cleavable *bis*-diazirine crosslinker strategy for reprocessing thermosets.

reformation under external stimuli (e.g., acid, base, fluoride etc.), thereby allowing low-functionality commodity polymers to be reversibly crosslinked through strong—yet selectively cleavable—covalent bonds. As with other *bis*-diazirines, the suite of reagents described herein can be topically applied to manufactured polymer materials without the need to melt or dissolve the polymer substrate. The addition of a cleavable group adds the potential for thermoset reprocessibility, together with facile polymer functionalization.

Results and Discussion

Design and synthesis of cleavable crosslinkers

Carbonate functional groups have been widely used in polymeric networks to establish reprocessable materials that can be degraded using specific chemical stimuli such as hydroxide or alkoxide anions.[18] Meanwhile, oxalate linkages, which benefit from higher rates of cleavage, have also been built into polymer materials.[19a] These have been investigated for certain medical applications, such as drug delivery and medical sutures.[19b] Silyl ether linkages have likewise been found to serve as robust and thermally stable sites in polymeric materials, which can be cleaved following the addition of acid or fluoride reagents. Such linkages can even be dynamic in nature, when amine groups are positioned nearby to facilitate fast exchange.[20]

We therefore set out to prepare a collection of cleavable crosslinkers with carbonate, oxalate, or silyl ether linkages installed between two electron-rich trifluoromethyl aryl diazirine warheads (**4**–**6**, Scheme 1b). Traditionally, *bis*-, *tetrakis*-, or *poly*-diazirine crosslinkers have either been made by functionalizing a suitable precursor with a commercially available diazirine-containing benzyl bromide,[13e–g,21] benzyl alcohol,[13d,14a,b] or benzoic acid[22] (in which case the synthesis is straightforward, but the product does not contain electronically optimized diazirine groups) or else by first derivatizing a desirable aromatic core with trifluoromethyl ketone groups and then elaborating the resulting product through a tedious sequence of oxime formation (using hydroxylamine), activation (using either tosyl chloride or nosyl chloride), diaziridine formation (through addition of ammonia) and finally oxidation to afford the desired diazirine.[13a–c,14c–e,17b] This latter approach allows one to exert more control over both the diazirine warhead and the linker group. However, it necessarily means that each new diazirine reagent requires a 6–8 step linear synthesis (Scheme S1). Seeking a faster and more efficient route to access the suite of cleavable crosslinkers proposed here, we recognized that the parent trifluoromethyl phenyl diazirine (**1**, Figure 1) was widely available, and could be sourced for as low as US$ 2/gram on multi-kilogram scale. We were therefore attracted to the idea of functionalizing precursor **1** with a *para*-linked ethereal tether. As discussed above, the use of an electron-rich aromatic group (which would be established through the addition of the *para*-oxygen) helps to stabilize the singlet carbene following diazirine activation,[23] which in turn affords up to 10-fold more efficient C–H insertion than is observed using electron-neutral or electron-poor trifluoromethyl aryl diazirines.[17a] If the ether linkage were to terminate in a functional group handle, this could then be exploited for the ready introduction of the desired carbonate, oxalate, and silyl ether cleavage sites.

While more step-economical than previous syntheses of electron-rich *bis*-diazirines, this approach introduced an additional synthetic challenge: because trifluoromethyl aryl diazirines containing *para*-alkoxy groups on the aromatic

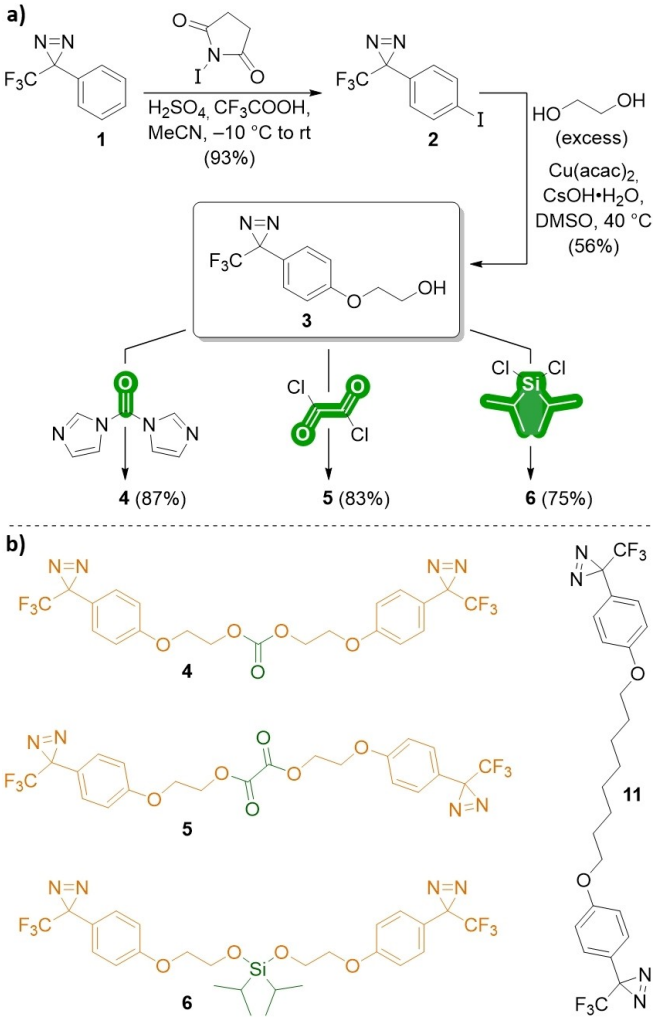

Scheme 1. Crosslinker design. a) Synthesis of cleavable crosslinkers from a common, readily accessible key intermediate. b) Structures of cleavable and non-cleavable *bis*-diazirine crosslinkers used in the present study.

ring decompose above ca. 40 °C, we were unable to harness palladium couplings to install the key aryl-oxygen bond, without resorting to prohibitively expensive ligand sets. Fortunately, we found that a low-temperature copper coupling based upon methodology from the Chae and Sun groups[24] provided an efficient and cost-effective solution.

In the event, treatment of **1** with *N*-iodosuccinimide in a mixture of trifluoroacetic acid, acetonitrile, and sulfuric acid[25] afforded *para*-iodo functionalized aryl diazirine (**2**) on >100 gram scale in 93 % yield (Scheme 1a). Subsequent reaction of **2** with excess ethylene glycol at 40 °C was facilitated by the use of recrystallized $Cu(acac)_2$, completing an efficient 2-step synthesis of key intermediate **3**, which had previously been prepared from 4-bromophenol over 7 steps, using the more traditional diazirine-construction sequence outlined above.[26] Cleavable crosslinkers **4–6** were then easily synthesized by subjecting glycol **3** to standard conditions for carbonate, oxalate, or silyl ether synthesis (refer to the Supporting Information for full details).

Evaluation of crosslinking-decrosslinking activity using a molecular model

To determine if our proposed method of introducing cleavable groups via *bis*-diazirine reagents would be useful for crosslinking and decrosslinking low-functionality materials, we first explored the use of a molecular model. Cyclohexane was chosen as a convenient surrogate for aliphatic polyolefins, since (like polyethylene) it contains only non-activated methylenes.

As reported previously, electronically optimized (but non-cleavable) *bis*-diazirine **11** (Scheme 1b) can crosslink this challenging substrate upon thermal or photochemical (395 nm) activation.[17b] The isolated yield of the pure *bis*-cyclohexane adduct from **11** was 91 % when the reaction was conducted at 140 °C, which is 10-fold better than a prototypical electron-poor diazirine-based crosslinker.[17b] When reacted at 90 °C for two hours, **11** still efficiently provided 82 % conversion. Repeating this experiment with **4–6** at 110 °C for one hour, we found that crosslinkers **4** and **6** performed similar to **11**, giving the carbonate-linked cyclohexane adduct **7** and silyl-linked **9** in 80 % conversion (Scheme 2). Although crosslinker **5** has poor solubility in cyclohexane, it still proceeds with >70 % conversion under the same reaction conditions, to afford the desired oxalate adduct, **8**. Photo-activation at 395 nm provided similar percent conversions; refer to the Supporting Information for full details.

To preliminarily assess the hydrolysis conditions and follow the reaction spectroscopically for each *bis*-adduct, compounds **7–9** were dissolved in CD_3OD, and aqueous NaOH was added directly to the NMR tube. After 4 hours, 90 % of compound **7** hydrolyzed to afford free alcohol **10** (Figure 2). By contrast, compound **9** showed only 2 % hydrolysis under same basic conditions. On the other hand, when the crosslinked cyclohexane adducts were exposed to

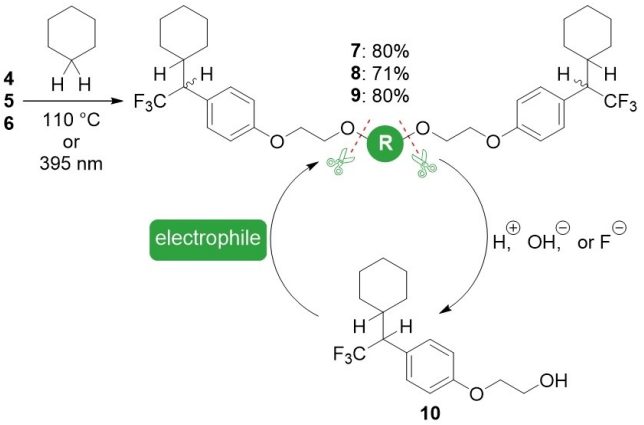

Scheme 2. Comparison of cyclohexane crosslinking efficacy and hydrolysis/regeneration of the resulting crosslink. Values for the cyclohexane insertion step indicate percent conversion to **7–9** (as diastereomeric mixtures) following thermal activation of the diazirine reagents. For isolated yields after column chromatography (which were slightly lower due to the sensitivity of the cleavable group), and for results following photochemical activation, refer to the Supporting Information.

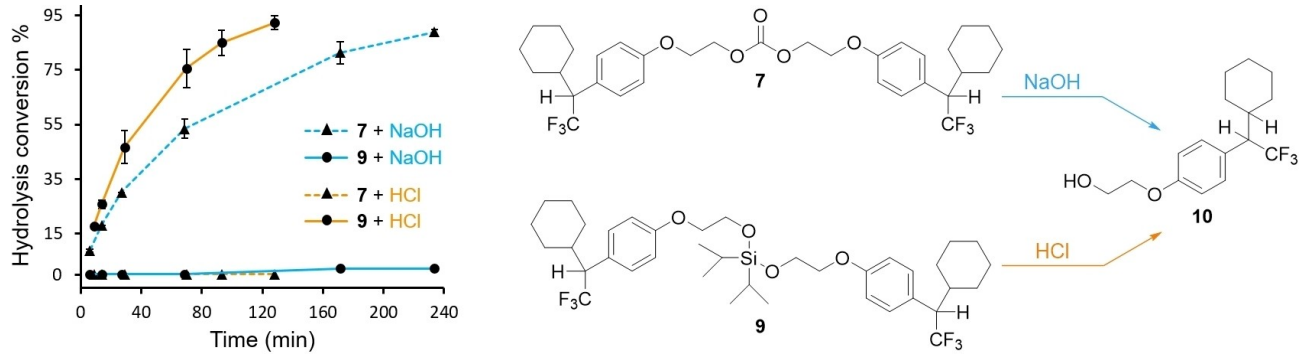

Figure 2. Hydrolysis of cyclohexane adducts **7** and **9** under basic (NaOH) and acidic (HCl) conditions. All experiments were performed directly in NMR tubes at room temperature, and use CD_3OD as solvent.

aqueous HCl in CD_3OD, silyl ether **9** hydrolyzed within 3 hours, but carbonate **7** remained unreacted. In both basic and acid conditions, oxalate **8** hydrolyzed within 15 minutes (refer to the Supporting Information for additional discussion). To demonstrate circularity in our molecular model, we directly added carbonyldiimidazole (CDI) into a suspension of compound **10** and K_2CO_3 in acetonitrile, to successfully reform the carbonate-linked *bis*-adduct **7** in quantitative conversion. Adducts **7–10** were isolated and fully characterized following each experiment; refer to the Supporting Information for spectroscopic details.

Polymeric models for evaluation of crosslinking and decrosslinking activity

To evaluate the suitability of the cleavable crosslinkers for reprocessing of low-functionality plastics via *crosslink-decrosslink-recrosslink* cycles, paraffin wax (PW; m.p. 58–62 °C; estimated M_r ca. 440) was chosen to facilitate rapid and accurate characterization by gel permeation chromatography (GPC). We firstly compared the effectiveness of all four crosslinkers (**4–6**, plus compound **11** as a non-cleavable control) in crosslinking paraffin wax. As evidenced by the presence of a higher molecular weight shoulder at 19–20 mins in the GPC traces (Figure 3a), each *bis*-diazirine reagent was capable of crosslinking the polymer.

We observed that crosslinkers **6** and **11**, containing less-polar tethers, crosslinked paraffin more efficiently than did **4** and **5**, which have more-polar tethers. This was evidenced by both a decreased retention time for the GPC peak associated with the crosslinked polymer, and a higher intensity for that same signal (Figure 3a). The incompatibility between the polar tether of crosslinkers **4** and **5** and the lipophilic polymer substrate results in phase separation (Figure S17) which leads to the lower crosslinking efficacy. Changing the polymer substrate to poly(ethylene glycol) (PEG; m.p. 44–48 °C; M_r ca. 1500), crosslinkers **5** and **11** showed similar crosslinking efficacy (Figure 3e) and there was no visible difference between the crosslinked polymer samples (Figure S17). By increasing the crosslinker loading from 10 to 20 mol %, the crosslinking efficacy changes similarly for both crosslinkers (i.e. compare Figure 3e and f).

Decrosslinking procedures were then applied to each crosslinked material. The paraffin wax samples crosslinked with **4** and **5** (i.e. PW-X-**4** and PW-X-**5**) were rapidly degraded by the addition of dilute NaOH (ca. 140 mM) to a solution of polymer in a mixture of tetrahydrofuran and methanol. Paraffin that had been treated with silyl ether **6** (PW-X-**6**) was treated with an equivalent concentration of dilute HCl (refer to the Supporting Information for full details). GPC analysis of the crude products showed complete degradation of the crosslinked polymers to the original molecular weight with no residual high MW shoulder (Figure 3b and c). As expected, paraffin wax crosslinked with **11** (PW-X-**11**; employed as a negative control for the decrosslinking step) did not hydrolyze under basic or acidic conditions. The sample of PEG that was crosslinked with compound **5** (i.e. PEG-X-**5**) was also successfully degraded into its original size under basic conditions (Figure 3e and f); once again the negative control sample (PEG-X-**11**) was unaffected by the addition of NaOH.

Functionalization and recrosslinking

Following decrosslinking, the pendant OH groups remaining on the paraffin wax provide the opportunity for recrosslinking or other modification. To demonstrate recrosslinking, the electrophile CDI was added directly to the decrosslinked paraffin wax samples, coupling nearby hydroxyl groups to reform a carbonate linkage. GPC analysis showed the reappearance of the high MW shoulder indicative of crosslinking (Figure 3d).

While the *crosslink-decrosslink-recrosslink* cycle illustrated thus far affords a potentially useful means of shuttling between thermoplastic and thermoset states within a given polymer material, we were also attracted to the potential to add new functionality to the hydroxyl-containing decrosslinked thermoplastic intermediate. To explore this possibility, we chose to add diazirine groups directly to hydrolyzed PW-X-**4**. To this end, a sample of paraffin wax was first crosslinked with 10 mol % of crosslinker **4**, and the formation of the carbonate-containing crosslink was confirmed by ^1H NMR (Figure 4). The sample was then hydrolyzed

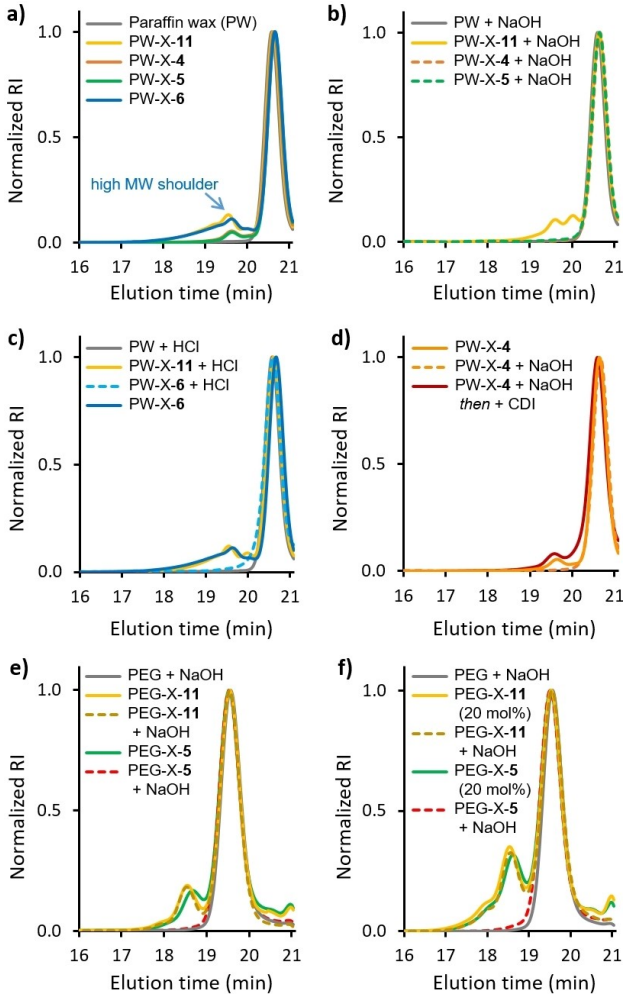

Figure 3. GPC traces of polymer samples after crosslinking/decrosslinking. a) Paraffin wax (PW) crosslinked (X) with 10 mol% *bis*-diazirine **4**, **5**, **6** or **11**, compared to native paraffin wax (vehicle control). b) Paraffin wax crosslinked with 10 mol% **4** or **5** treated with NaOH and compared to negative and vehicle controls. c) 10 mol% **6**-doped paraffin wax treated with HCl and compared to negative and vehicle controls. d) Decrosslinked paraffin wax (containing pendant OH groups) reacted with CDI to achieve recrosslinking. e) 10 mol% **5** or **11** (negative control)-doped PEG before and after NaOH treatment. f) 20 mol% **5** or **11**-doped PEG before and after NaOH treatment. RI, refractive index. Vehicle control samples were prepared identically to the test samples, but without the addition of crosslinker.

through the addition of NaOH, and once again the successful transformation was confirmed spectroscopically. Finally, an excess of diazirine-containing benzyl bromide was added, and (after washing away excess electrophile), the formation of the labeled product was confirmed by both ^{1}H NMR spectroscopy and DSC (Figures S41 and S42).

Application to commercial low-functionality polyolefins

To translate the results on cyclohexane and paraffin wax to more challenging polymeric substrates, isotactic polypropylene (iPP; M_n ca. 5000 g mol^{-1}) was selected as a representative low-functionality plastic. Of the three cleavable crosslinkers investigated above, oxalate-linked compound **5** appeared to contain the most labile linkage. We therefore added 10 wt% of crosslinker **5** or **11** (as a non-cleavable control) to commercial iPP, and thermally activated the sample (110 °C for 2 hours) to initiate crosslinking. Thermal properties for the samples (as well as those of the relevant vehicle control) were then analyzed by differential scanning calorimetry (DSC). As expected, both of the crosslinked polymer samples demonstrated decreased enthalpies in the melting transition, when compared to the vehicle control sample. These enthalpy decreases, where crosslinked regions of the polymer structure behave as thermosets and therefore no longer melt,[2a,13b] were consistently displayed in both the heating and cooling cycles of each DSC trace (Table 1). To test the reprocessability of crosslinked iPP samples, aqueous NaOH was mixed with the iPP substrates (refer to the Supporting Information for full details). As anticipated, the iPP sample that had been crosslinked with **5** afforded the same enthalpy values as the vehicle control sample following the decrosslinking procedure—indicating successful rescue of thermoplastic properties. Conversely, the iPP sample crosslinked with **11** maintained its reduced crystallization and fusion enthalpies, indicating that no decrosslinking had taken place within the negative control.

To explore the effect of crosslinking and decrosslinking on *mixtures* of aliphatic polymers, we added crosslinkers **4**–**6**, as well as non-cleavable crosslinker **11**, at 10 wt% loading, to a 1:1 mixture of polyethylene (PE; m.p. 92 °C; M_n ca. 1700 g mol^{-1}) and iPP (m.p. 157 °C; M_n ca. 5000 g mol^{-1}). Once again we observed a consistent decrease in the enthalpy associated with the melting and crystallization transitions (Table 2), with the three cleavable crosslinkers performing more efficiently than non-cleavable *bis*-diazirine **11**. Reprocessability of these new thermoset materials was then demonstrated by hydrolyzing them back into their thermoplastic states. Basic conditions were employed for

Table 1: Evolution of thermal properties of crosslinked polypropylene before and after hydrolysis.

Sample	$\Delta H_{crystal}$ (J/g)[a]	ΔH_{fusion} (J/g)[b]
iPP$_{(vehicle\ control)}$	94.9	99.8
iPP-X-**5**	81.7 (86%)	86.3 (86%)
iPP-X-**11**	77.6 (82%)	82.9 (83%)
iPP$_{(vehicle\ control)}$ + NaOH	96.0	100.1
iPP-X-**5** + NaOH	96.6 (101%)	101.8 (106%)
iPP-X-**11** + NaOH	82.1 (86%)	86.9 (87%)

[a] The integrated region for crystallization enthalpy was from 90 to 150 °C. [b] The fusion enthalpy was determined from the second heating cycle and integrated from 90 to 170 °C. Percentage values (shown in parentheses) are defined relative to the appropriate vehicle control.

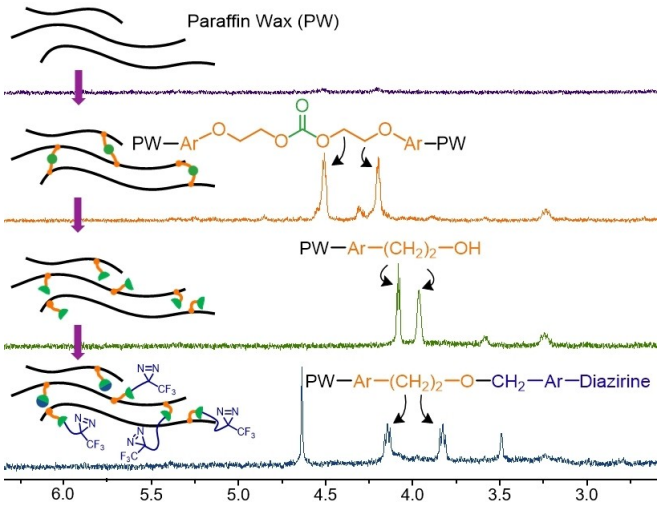

Figure 4. Stacked ^{1}H NMR spectra indicating the functionalization of a hydrolyzed (decrosslinked) paraffin wax sample reacted with a benzyl bromide-containing diazirine. All spectra were recorded in $CDCl_3$. See Figure S41 for integrations.

samples crosslinked with **4** and **5**, while tetrabutylammonium fluoride (TBAF) was used for samples crosslinked with **6**. As expected, the crystallization and fusion enthalpies for samples crosslinked with **4**–**6** returned to nearly the values associated with the corresponding vehicle control samples, while samples crosslinked with non-cleavable control **11** maintained lower enthalpies—indicating resistance to hydrolysis conditions.

Application to reversible PDMS crosslinking

To demonstrate curing in a representative liquid polymer matrix, we applied polydimethylsiloxane (PDMS; viscosity 18000–22000 cSt) containing 5 wt % of *bis*-diazirine **4** to a rheometer stage for direct measurement of the change in storage modulus during crosslinking. As anticipated, we observed a pronounced increase in shear modulus as the sample passed beyond the activation temperature for **4** (Figure S63). A PDMS control sample, by contrast, showed no such modulus increase upon heating.

We also crosslinked bulk PDMS with **4**, and then decrosslinked the sample by addition of NaOH. As expected, crosslinked PDMS was a mechanically stable gel, while the decrosslinked sample regained the ability to flow with gravity (Figure S62 and Movie S1).

Thermomechanical testing of crosslinked polymers

To assess the effective crosslink density within a representative commercial polyolefin treated with a cleavable crosslinker, 5 wt % of carbonate crosslinker **4** was added to injection-moulding grade low-density polyethylene (LDPE; melt flow rate 21). After thermal activation and melt-

Table 2: Enthalpy analysis of crosslinked and decrosslinked mixed-polyolefin plastics.

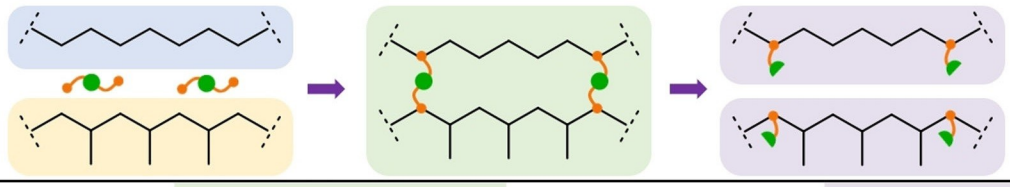

	Following crosslinking			Following decrosslinking	
Sample	$\Delta H_{crystal}$ (J/g)[a]	ΔH_{fusion} (J/g)[b]	Sample	$\Delta H_{crystal}$ (J/g)[a]	ΔH_{fusion} (J/g)[b]
iPP/PE$_{(vehicle\ control)}$	88.8	90.7	iPP/PE$_{(vehicle\ control)}$ + NaOH	83.3	85.3
iPP/PE-X-**11**[c]	79.1 (89%)	79.8 (88%)	iPP/PE-X-**11** + NaOH	69.6 (84%)	69.8 (82%)
iPP/PE-X-**4**[d]	66.1 (74%)	65.5 (72%)	iPP/PE-X-**4** + NaOH	78.0 (94%)	80.3 (94%)
iPP/PE-X-**5**[d]	70.2 (79%)	71.5 (79%)	iPP/PE-X-**5** + NaOH	79.1 (95%)	82.2 (96%)
iPP/PE$_{(vehicle\ control)}$	88.8	90.7	iPP/PE$_{(vehicle\ control)}$ + TBAF	105.7	110.0
iPP/PE-X-**11**[c]	79.1 (89%)	79.8 (88%)	iPP/PE-X-**11** + TBAF	87.1 (82%)	93.9 (85%)
iPP/PE-X-**6**[d]	68.7 (77%)	69.2 (76%)	iPP/PE-X-**6** + TBAF	101.8 (96%)	104.4 (95%)

[a] The integrated region for crystallization enthalpy was from 50 to 120 °C. [b] The fusion enthalpy was determined from the second heating cycle and integrated from 50 to 170 °C. Percentage values (shown in parentheses) are defined relative to the appropriate vehicle control. [c] A mixture of isotactic polypropylene (iPP) and polyethylene (PE) were reacted with non-cleavable crosslinker **11**, as a negative control for the decrosslinking experiment. [d] A mixture of iPP and PE were reacted with the indicated cleavable crosslinker.

processing to generate regular-dimensioned macro-scale objects (refer to the Supporting Information for details), crosslinked samples (or vehicle controls, prepared identically but with no added crosslinker) were extracted with hot toluene to determine the gel content,[7,27a] and were subjected to dynamic mechanical thermal analysis (DMTA) to measure the average apparent molecular weight difference between crosslinks ($M_{c,a}$).

Despite the low loading of *bis*-diazirine **4**, crosslinked LDPE samples were found to have a gel content of 95±3% (compared with 0% gel content for the corresponding vehicle control samples). Perhaps most significantly, DMTA analysis of the crosslinked samples revealed a pronounced rubbery plateau above ca. 125 °C, confirming that these samples had been transformed into thermosets (Figure 5b). The corresponding vehicle control samples, by contrast, behaved as pure thermoplastics, exhibiting clean melting transitions at elevated temperature (Figure 5a).

The rubbery plateau for LDPE samples crosslinked with 5 wt% of **4** corresponds to storage modulus of 0.414± 0.010 MPa. Calculating the $M_{c,a}$ from this value using the theory of rubbery elasticity[27] and the measured sample density (0.936±0.007 g cm^{-3}) revealed a distance between mechanically productive crosslinks of approximately 23300 g mol^{-1} (i.e. 1660 methylene units between crosslink points). Comparison to the total number of C–H insertion events expected for **4** within a polyethylene matrix (based on the cyclohexane model experiments discussed above; refer to the Supporting Information for calculations) suggests a ratio of productive crosslinks (where **4** bridges two polyethylene chains) to unproductive loops (where **4** reacts twice on the same chain) of approximately 1:2.5. A distinct rubbery plateau was also observed for LDPE samples crosslinked with only 2 wt% of **4** (see Figure S49). While this necessarily occurs at a lower storage modulus (ca. 0.12 MPa) due to the very low ratio of crosslinker molecules to LDPE methylene units, it nevertheless provides compelling evidence for the ability of small-molecule *bis*-diazirines to imbue thermoplastic materials with thermoset-like performance characteristics.

We next prepared melt-processed mixtures of LDPE and amorphous polypropylene (aPP), in which the samples were either treated with 5 wt% of *bis*-diazirine **4** or a solvent blank. Once again, the vehicle controls showed melting transitions consistent with thermoplastic behavior (Figure 5c), while the samples treated with **4** displayed stable rubbery plateaus consistent with their conversion to thermosets. The plateau modulus was lower than that observed for the crosslinked pure LDPE samples in Figure 5b, indicating a lower density of mechanically productive crosslinks. This decrease in performance is reflective of the challenge inherent in crosslinking immiscible materials, and was also reflected in a reduced gel content for the crosslinked mixture of LDPE+aPP (73±6%), compared with that discussed above for crosslinked LDPE. Nevertheless, the existence of a stable and consistent rubbery plateau in these samples (together with complementary microscopy and tensile data available in Figures S53 and S59) provided good evidence that some portion of crosslinks within the material were occurring at the LDPE:aPP interface. By contrast, control samples prepared from pre-crosslinked LDPE and pre-crosslinked aPP (in which both homopolymers are individually crosslinked, but where no crosslinking is possible at the interface) performed poorly and irreproducibly in DMTA testing (Figure S61a).

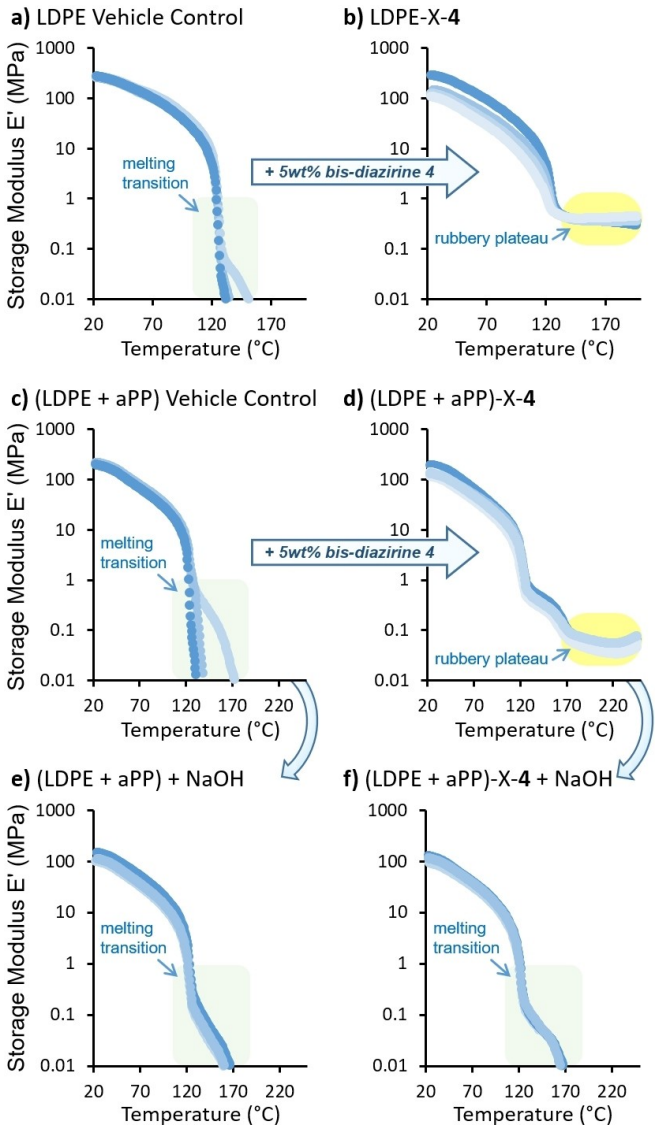

Figure 5. DMTA curves for polymer samples after crosslinking/decrosslinking. a) Vehicle control samples prepared from low-density polyethylene (LDPE). b) LDPE samples crosslinked with 5 wt% *bis*-diazirine **4**. c) Vehicle control samples prepared from a 1:1 mixture (by weight) of amorphous polypropylene (aPP) and LDPE. d) aPP:LDPE samples crosslinked with 5 wt% *bis*-diazirine **4**. e) aPP:LDPE samples treated with NaOH. f) crosslinked aPP:LDPE samples (prepared identically to those tested in panel d), then treated with NaOH to trigger decrosslinking. Replicate samples are indicated in differing shades of blue; at least 3 samples were tested for each condition. Melting behavior is highlighted in light green. Rubbery plateau regions are highlighted in yellow. Refer to Tables S9 and S12 for collected DSC and WAXS data for crosslinked polymers; no significant differences in percent crystallinity were observed, even when the enthalpy of melting was substantively reduced.

Finally, to demonstrate the ability to convert the crosslinked LDPE:aPP thermoset composite back into a mixture of thermoplastics, we subjected (LDPE + aPP)-X-**4** samples to hydrolysis conditions. This served to remove the rubbery plateau (compare Figure 5f to Figure 5d), giving samples that performed identically to the corresponding vehicle controls (compare Figure 5f to Figure 5e).

Conclusion

A series of simple, yet powerful, cleavable crosslinkers has been introduced that can be used to upcycle low-functionality thermoplastic materials into reprocessable thermosets. Cleavage of the labile linker groups can be accomplished using a range of external stimuli (base, acid, or fluoride), and the decrosslinked polymer products resulting from these operations contain pendent hydroxyl groups that can either be used for recrosslinking or further functionalization.

The opportunity to crosslink mixtures of incompatible polymers (e.g. polyethylene and polypropylene) together to form novel covalent composites is particularly attractive, given the persistent problem of mixed plastic waste streams. Polyethylene is frequently contaminated with polypropylene, and polypropylene is even more frequently contaminated with polyethylene.[28] Simple melt-blending of these mixed materials leads to poor mechanical properties due to phase separation,[29] and cross-contamination challenges of this type are partially responsible for the fact that only 9 % of all plastics ever produced have been recycled.[4] Because small-molecule *bis*-diazirines react promiscuously with polymer substrates and cannot easily distinguish between different polymer architectures, they readily connect dissimilar polymers.[13c] Together with other recently disclosed reagents for functionalization of commodity polymers through reaction at C–H bonds,[30] the cleavable crosslinkers described herein may provide a useful means of generating reprocessable thermosets from low-functionality thermoplastics and post-consumer waste.

Acknowledgements

We gratefully acknowledge Mitacs Canada (grant IT17318) for fellowships and consumables support to L.B., and thank XlynX Materials for operating funds that were used to support this research. L.B. thanks the University of Victoria for Nora & Mark Degoutiere Memorial, David McGillivray, and Dr. Wilma Elias Graduate Scholarships. J.W. additionally thanks the Canada Research Chairs program (file number 950-231376) for salary support. Finally, we thank Dr. Stefania F. Musolino for helpful discussions, Madisen MacFarlane for conducting tensile measurements, and the Advanced Microscopy Facility at the University of Victoria for assistance acquiring the SEM images.

Conflict of Interest

Authors J.W. and L.B. are co-authors on a patent (63/158,578) claiming the use of crosslinkers described in the current work. There are no additional conflicts.

Data Availability Statement

The data that support the findings of this study are available in the Supporting Information of this article.

Keywords: Diazirines · Polymer Crosslinking · Polymer Functionalization · Polymer Processing · Thermosets

[1] S. Ma, D. C. Webster, *Prog. Polym. Sci.* **2018**, *76*, 65–110.
[2] a) H. A. Khonakdar, J. Morshedian, U. Wagenknecht, S. H. Jafari, *Polymer* **2003**, *44*, 4301–4309; b) A. Rahimi, J. M. García, *Nat. Chem. Rev.* **2017**, *1*, 0046.
[3] a) D. J. Fortman, J. P. Brutman, G. X. De Hoe, R. L. Snyder, W. R. Dichtel, M. A. Hillmyer, *ACS Sustainable Chem. Eng.* **2018**, *6*, 11145–11159; b) W. Post, A. Susa, R. Blaauw, K. Molenveld, R. J. I. Knoop, *Polym. Rev.* **2020**, *60*, 359–388.
[4] a) Chemical Sciences and Society Summit, *Science to Enable Sustainable Plastics*, London, UK, **2020**, https://rsc.li/progressive-plastics-report; b) R. Geyer, J. R. Jambeck, K. L. Law, *Sci. Adv.* **2017**, *3*, e1700782.
[5] P. Shieh, W. Zhang, K. E. L. Husted, S. L. Kristufek, B. Xiong, D. J. Lundberg, J. Lem, D. Veysset, Y. Sun, K. A. Nelson, D. L. Plata, J. A. Johnson, *Nature* **2020**, *583*, 542–547.
[6] D. T. Sheppard, K. Jin, L. S. Hamachi, W. Dean, D. J. Fortman, C. J. Ellison, W. R. Dichtel, *ACS Cent. Sci.* **2020**, *6*, 921–927.
[7] P. R. Christensen, A. M. Scheuermann, K. E. Loeffler, B. A. Helms, *Nat. Chem.* **2019**, *11*, 442–448.
[8] M. Röttger, T. Domenech, R. van der Weegen, A. Breuillac, R. Nicolaÿ, L. Leibler, *Science* **2017**, *356*, 62–65.
[9] J. Kruželák, R. Sýkora, I. Hudec, *Chem. Pap.* **2016**, *70*, 1533–1555.
[10] A. V. Radchenko, F. Ganachaud, *Ind. Eng. Chem. Res.* **2022**, *61*, 7679–7698.
[11] M. J. Marks, R. Vernon Snelgrove, *ACS Appl. Mater. Interfaces* **2009**, *1*, 921–926.
[12] a) I. Chodák, *Polymer Science and Technology Series, Vol. 2* (Ed.: J. Karger-Kocsis), Springer Netherlands, Dordrecht, **1999**, pp. 128–134; b) J. Thomas, B. Joseph, J. P. Jose, H. J. Maria, P. Main, A. Ali Rahman, B. Francis, Z. Ahmad, S. Thomas, *Ind. Eng. Chem. Res.* **2019**, *58*, 20863–20879.
[13] a) A. Blencowe, C. Blencowe, K. Cosstick, W. Hayes, *React. Funct. Polym.* **2008**, *68*, 868–875; b) M. L. Lepage, C. Simhadri, C. Liu, M. Takaffoli, L. Bi, B. Crawford, A. S. Milani, J. E. Wulff, *Science* **2019**, *366*, 875–878; c) C. Simhadri, L. Bi, M. L. Lepage, M. Takaffoli, Z. Pei, S. F. Musolino, A. S. Milani, G. A. DiLabio, J. E. Wulff, *Chem. Sci.* **2021**, *12*, 4147–4153; d) P. Bexis, M. C. Arno, C. A. Bell, A. W. Thomas, A. P. Dove, *Chem. Commun.* **2021**, *57*, 4275–4278; e) T. J. Cuthbert, S. Ennis, S. F. Musolino, H. L. Buckley, M. Niikura, J. E. Wulff, C. Menon, *Sci. Rep.* **2021**, *11*, 19029; f) R. Nazir, L. Bi, S. F. Musolino, O. H. Margoto, K. Çelebi, C. Mobuchon, M. Takaffoli, A. S. Milani, G. Falck, J. E. Wulff, *ACS Appl. Polym. Mater.* **2022**, *4*, 1728–1742; g) M. Singh, C. E. Varela, W. Whyte, M. A. Horvath, N. C. S. Tan, C. B. Ong, P. Liang, M. L. Schermerhorn, E. T. Roche, T. W. J. Steele, *Sci. Adv.* **2021**, *7*, eabf6855.

[14] a) H. Burgoon, C. Cyrus, D. Skilskyj, J. Thoresen, C. Ebner, G. A. Meyer, P. Filson, L. F. Rhodes, T. Backlund, A. Meneau, T. Cull, I. Afonina, *ACS Appl. Polym. Mater.* **2020**, *2*, 1819–1826; b) Y.-Q. Zheng, Y. Liu, D. Zhong, S. Nikzad, S. Liu, Z. Yu, D. Liu, H.-C. Wu, C. Zhu, J. Li, H. Tran, J. B.-H. Tok, Z. Bao, *Science* **2021**, *373*, 88–94; c) K. Dey, S. R. Chowdhury, E. Dykstra, A. Koronatov, H. P. Lu, R. Shinar, J. Shinar, P. Anzenbacher, *J. Mater. Chem. C* **2020**, *8*, 11988–11996; d) C. Wu, C. Li, X. Yu, L. Chen, C. Gao, X. Zhang, G. Zhang, D. Zhang, *Angew. Chem. Int. Ed.* **2021**, *60*, 21521–21528; e) S. Lu, Z. Fu, F. Li, K. Weng, L. Zhou, L. Zhang, Y. Yang, H. Qiu, D. Liu, W. Qing, H. Ding, X. Sheng, M. Chen, X. Tang, L. Duan, W. Liu, L. Wu, Y. Yang, H. Zhang, J. Li, *Angew. Chem. Int. Ed.* **2022**, *61*, e202202633.

[15] a) J. Brunner, H. Senn, F. M. Richards, *J. Biol. Chem.* **1980**, *255*, 3313–3318; b) C. P. Seath, A. D. Trowbridge, T. W. Muir, D. W. C. MacMillan, *Chem. Soc. Rev.* **2021**, *50*, 2911–2926.

[16] T. Ollevier, V. Carreras, *ACS Org. Inorg. Au* **2022**, *2*, 83–98.

[17] a) S. F. Musolino, Z. Pei, L. Bi, G. A. DiLabio, J. E. Wulff, *Chem. Sci.* **2021**, *12*, 12138–12148; b) S. F. Musolino, M. Mahbod, R. Nazir, L. Bi, H. A. Graham, A. S. Milani, J. E. Wulff, *Polym. Chem.* **2022**, *13*, 3833–3839.

[18] a) M. Häußler, M. Eck, D. Rothauer, S. Mecking, *Nature* **2021**, *590*, 423–427; b) P. G. Maschmeyer, X. Liang, A. Hung, O. Ahmadzai, A. L. Kenny, Y. C. Luong, T. N. Forder, H. Zeng, E. R. Gillies, D. A. Roberts, *Polym. Chem.* **2021**, *12*, 6824–6831.

[19] a) J. J. Garcia, S. A. Miller, *Polym. Chem.* **2014**, *5*, 955–961; b) C.-C. Song, F.-S. Du, Z.-C. Li, *J. Mater. Chem. B* **2014**, *2*, 3413–3426.

[20] a) M. Barth, R. Fischer, R. Brock, J. Rademann, *Angew. Chem. Int. Ed.* **2005**, *44*, 1560–1563; b) M. C. Parrott, J. C. Luft, J. D. Byrne, J. H. Fain, M. E. Napier, J. M. DeSimone, *J. Am. Chem. Soc.* **2010**, *132*, 17928–17932; c) Y. Nishimura, J. Chung, H. Muradyan, Z. Guan, *J. Am. Chem. Soc.* **2017**, *139*, 14881–14884; d) P. Shieh, H. V.-T. Nguyen, J. A. Johnson, *Nat. Chem.* **2019**, *11*, 1124–1132.

[21] J. Ping, F. Gao, J. L. Chen, R. D. Webster, T. W. J. Steele, *Nat. Commun.* **2015**, *6*, 8050.

[22] a) A. Welle, F. Billard, J. Marchand-Brynaert, *Synthesis* **2012**, *44*, 2249–2254; b) I. Djordjevic, G. Wicaksono, I. Solic, T. W. J. Steele, *Macromol. Rapid Commun.* **2020**, *41*, 2000235.

[23] a) M.-G. Song, R. S. Sheridan, *J. Am. Chem. Soc.* **2011**, *133*, 19688–19690; b) B. Raimer, T. Lindel, *Chem. Eur. J.* **2013**, *19*, 6551–6555.

[24] a) Y. Liu, S. K. Park, Y. Xiao, J. Chae, *Org. Biomol. Chem.* **2014**, *12*, 4747–4753; b) Y. Zheng, W. Zou, L. Luo, J. Chen, S. Lin, Q. Sun, *RSC Adv.* **2015**, *5*, 66104–66108.

[25] M. Bergström, G. Suresh, V. R. Naidu, C. R. Unelius, *Eur. J. Org. Chem.* **2017**, *2017*, 3234–3239.

[26] C. Morita, K. Hashimoto, T. Okuno, H. Shirahama, *Heterocycles* **2000**, *52*, 1163–1169.

[27] a) C. He, P. R. Christensen, T. J. Seguin, E. A. Dailing, B. M. Wood, R. K. Walde, K. A. Persson, T. P. Russell, B. A. Helms, *Angew. Chem. Int. Ed.* **2020**, *59*, 735–739; b) T. R. Long, R. M. Elder, E. D. Bain, K. A. Masser, T. W. Sirk, J. H. Yu, D. B. Knorr, J. L. Lenhart, *Soft Matter* **2018**, *14*, 3344–3360; c) I. M. Barszczewska-Rybarek, A. Korytkowska-Wałach, M. Kurcok, G. Chladek, J. Kasperski, *Acta Bioeng. Biomech.* **2017**, *19*, 47–53.

[28] a) R. Juan, B. Paredes, R. A. García-Muñoz, C. Domínguez, *Polym. Test.* **2021**, *100*, 107273; b) E. Karaagac, M. P. Jones, T. Koch, V.-M. Archodoulaki, *Polymer* **2021**, *13*, 2618; c) E. Karaagac, T. Koch, V.-M. Archodoulaki, *Waste Manage.* **2021**, *119*, 285–294.

[29] a) S. Yin, R. Tuladhar, F. Shi, R. A. Shanks, M. Combe, T. Collister, *Polym. Eng. Sci.* **2015**, *55*, 2899–2909; b) D. Nwabunma, T. Kyu in *Polyolefin Blends* (Eds.: D. Nwabunma, T. Kyu), Wiley, Hoboken, **2007**, pp. 1–26; c) C. Jehanno, J. W. Alty, M. Roosen, S. De Meester, A. P. Dove, E. Y.-X. Chen, F. A. Leibfarth, H. Sardon, *Nature* **2022**, *603*, 803–814; d) J. M. Eagan, J. Xu, R. Di Girolamo, C. M. Thurber, C. W. Macosko, A. M. LaPointe, F. S. Bates, G. W. Coates, *Science* **2017**, *355*, 814–816.

[30] a) C. M. Plummer, L. Li, Y. Chen, *Polym. Chem.* **2020**, *11*, 6862–6872; b) C. M. Plummer, H. Zhou, S. Li, H. Zhong, Z. Sun, C. Bariashir, W.-H. Sun, H. Huang, L. Liu, Y. Chen, *Polym. Chem.* **2019**, *10*, 3325–3333; c) T. J. Fazekas, J. W. Alty, E. K. Neidhart, A. S. Miller, F. A. Leibfarth, E. J. Alexanian, *Science* **2022**, *375*, 545–550; d) R. W. Clarke, T. Sandmeier, K. A. Franklin, D. Reich, X. Zhang, N. Vengallur, T. K. Patra, R. J. Tannenbaum, S. Adhikari, S. K. Kumar, T. Rovis, E. Y.-X. Chen, *Nature* **2023**, *616*, 731–739.

Manuscript received: April 3, 2023
Accepted manuscript online: May 25, 2023
Version of record online: May 25, 2023